

A kilohertz nanosecond 1645 nm KTA-OPO pumped by a 1064 nm pulse laser for methane detection

Hanlin Jiang (姜涵林)^{1,2,3,†}, Chao Ma (马超)^{1,†}, Mingjian Wang (王明建)^{1,3*}, Zhenzhen Yu (于真真)¹, Yue Song (宋越)¹, Yan Feng (冯衍)^{2,3}, Shiguang Li (李世光)¹, Jiqiao Liu (刘继桥)^{1,3}, Xia Hou (侯霞)^{1,3}, and Weibiao Chen (陈卫标)^{1,2,3}

¹Wangzhijiang Innovation Center for Laser, Aerospace Laser Technology and System Department, Shanghai Institute of Optics and Fine Mechanics, Chinese Academy of Sciences, Shanghai 201800, China

²Hangzhou Institute for Advanced Study, University of Chinese Academy of Sciences, Hangzhou 310024, China

³Center of Materials Science and Optoelectronics Engineering, University of Chinese Academy of Sciences, Beijing 100190, China

[†]These authors contributed equally to this work.

*Corresponding author: wmjian@siom.ac.cn

Received September 24, 2024 | Accepted December 20, 2024 | Posted Online May 16, 2025

In this Letter, we studied a kilohertz nanosecond 1645 nm optical parametric oscillator (OPO) for methane detection. The OPO pump source was an electro-optical Q -switched 1064 nm oscillator, followed by a preamplifier and two Innoslab amplifiers. Two KTiOAsO_4 crystals with type II angular phase matching were used as the nonlinear working materials, and two plane mirrors were used for the OPO cavity. We achieved the signal light with an average power of 9.32 W and a minimum pulse duration of 1.8 ns at a repetition rate of 8 kHz for a 54.1 W pump power, and the optical-optical conversion efficiency was 17.3%. The beam quality was measured as $M_x^2 = 1.08$ and $M_y^2 = 1.22$. The wavelength of the signal light was continuously tunable from 1641.9207 to 1648.1791 nm. To the best of our knowledge, this is the highest average power achieved at the kilohertz regime of a 1645 nm laser.

Keywords: optical parametric oscillator; wavelength tuning; methane detection.

DOI: [10.3788/COL202523.061401](https://doi.org/10.3788/COL202523.061401)

1. Introduction

Methane, the second most potent greenhouse gas after carbon dioxide, accounted for 16% of global greenhouse gas emissions^[1]. To explore the impacts of methane gas on the Earth and humans, we need high-resolution spatial and temporal methane gas distributions and data^[2]. Active optical sensors based on the integrated path differential absorption (IPDA) lidar method were considered promising candidates for measuring carbon dioxide and methane to address carbon cycle science in all critical regions of the globe^[3–8]. The 1645 nm wavelength laser was located exactly at the peak absorption of methane gas, making it the most important and best laser wavelength for detecting atmospheric methane^[9].

Optical parametric oscillator (OPO) has been demonstrated to be a highly promising technique for the generation of infrared lasers, offering a lower pump power threshold, a higher conversion efficiency, a narrower spectrum, and a better beam quality. So far, many reports on KTA-OPO have focused on the 1.5–1.8 μm band^[10–14], such as the reported 143 W acousto-optic (AO) Q -switched Nd:YAG intracavity pumped 25 mm KTA crystal that obtained a 1534 nm signal light with an average

power of 5.35 W and a pulse duration of 3.71 ns at a 6 kHz repetition rate^[10]. Additionally, an 880 nm LD intracavity pumped Nd:YVO₄/KTA OPO was demonstrated for the generation of a 1533 nm signal light at 10 kHz, with an output of 2.6 W of a 3.5 μm signal light. The optical-optical conversion efficiency was determined to be 6.74%, and the beam quality was found to be 2.12.^[11] Other researchers employed the KTA and KTiOPO_4 to achieve a repetition rate of 4 kHz and a pulse duration of 10.5 ns, with a maximum total average power of 1.2 W for 1534 and 1572 nm signal lights^[12]. A ps regenerative amplifier operated OPO to achieve tunable signal light from 1501 to 1565 nm at 5 and 10 kHz, respectively, and obtained a 1532 nm signal light at 5 kHz with 21.6 μJ and 6 ps^[13]. A single-channel multi-stage optical parameter generation-optical parametric amplifier (OPG-OPA) was pumped by an 86 ps and 10 kHz 1064 nm picosecond laser, and obtained an average power of 502 mW, with a pulse energy of 50.2 μJ and a beam quality of 1.87×2.16 at 1770 nm^[14].

As for the 1645 nm, Livrozet *et al.*^[15] obtained a 25 Hz 0.233 W 1645 nm laser using a KTP crystal. Chen *et al.* developed an injection-seeded OPO using a 1064 nm single-frequency Nd:YAG master oscillator power amplifier (MOPA)

laser as the pump source^[16]. A distributed feedback (DFB) fiber laser with a linewidth of 3 MHz was used to pump the OPO. An input of 11 mJ pump pulse at a repetition rate of 50 Hz resulted in a signal pulse energy of 1.8 mJ. The OPO had a pulse duration of 15 ns and a corresponding linewidth of 45 MHz. But for the kHz and high power, a 1645 nm tunable laser with a high-beam-quality pump source has not been reported. In this Letter, we studied a kilohertz nanosecond 1645 nm OPO for methane detection.

2. Experimental Setup

The amplification process of the 1064 nm pump source in the 1645 nm OPO is illustrated in Fig. 1(a), which adopts a MOPA structure. The seed laser was an electro-optical Q-switched pulse laser end-pumped by the 808 nm LD and generated by the 1064 nm 10 kHz 1 W fundamental wavelength. Then, after pre-amplifier and two-stage Innoslab amplification, the 60.1 W 1064 nm laser was achieved as the pump source for the 1645 nm OPO, as shown in Fig. 1(b).

The 1645 nm KTA-OPO experimental setup diagram is shown in Fig. 1(b). A 1064 nm half-waveplate (HWP) and a 1064 nm polarization beam splitter (PBS) were employed to control the input pump power. Since the laser spot from Innoslab-2 was elliptical and the divergence angle in the vertical direction was larger than that in the horizontal direction, vertical

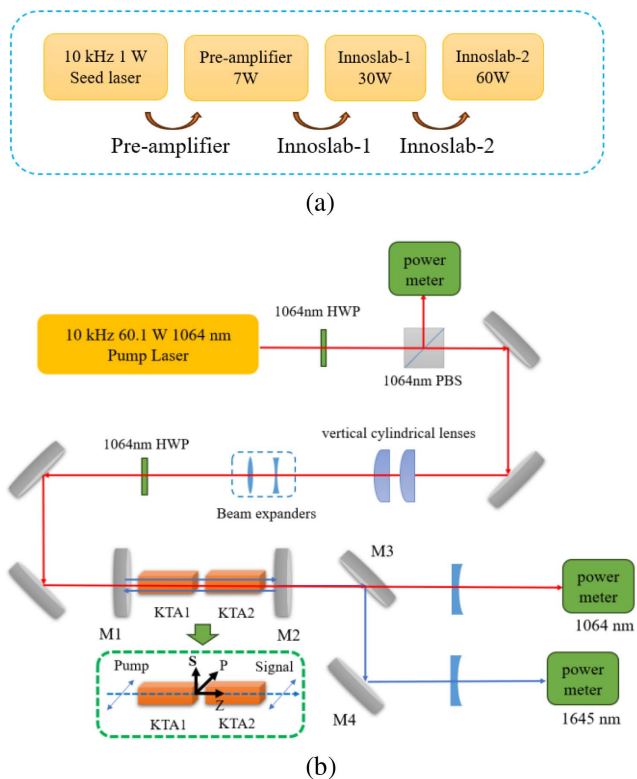


Fig. 1. (a) Schematic representation of the amplification process of the 1064 nm pump source. (b) Experimental setup diagram of the 1645 nm KTA-OPO.

cylindrical lenses were used to compress the vertical divergence, thereby ensuring that the angle of divergence in both horizontal and vertical directions was consistent, and the spot was shaped to be close to a nearly circular spot before entering the beam expanders. Then, the divergence angle at the position of the nearly circular spot was compressed using the beam expanders to make it meet the mode matching of the KTA-OPO. The polarization of the 1064 nm pump laser was adjusted to p-polarization by an HWP.

Using the thermal lens focal length formula, the equivalent focal length of a single KTA crystal under a 54.1 W 1064 nm pump source was calculated to be 906.1 mm. Subsequently, the reZonator software was employed to simulate the eigenmode when two thermal lens crystals were present within the OPO cavity. This revealed that the waist radius at the position of the cavity mirrors of M1 and M2 was 185.2 μm . Then, we adjusted the beam expanders and vertical cylindrical lenses to change the size and divergence angle of the pump spot to match the size of the OPO cavity mode. The beam waist position spot of the 54.1 W 1064 nm pump light was measured using a CCD camera (Ophir, SP920) with BeamGage Standard software, as shown in Fig. 2. The waist spot size of the pump beam was measured to be 490 $\mu\text{m} \times 322 \mu\text{m}$. The pulse duration of the pump light was 2.3 ns, the corresponding peak power of the pump light was calculated to be 2.94 MW, and the peak power density was 1.2 GW/cm^2 .

The KTA-OPO adopted a two-plane mirror configuration, as shown in Fig. 3. The cavity mirrors had high transmittance for the idler light to prevent the reverse conversion process in the

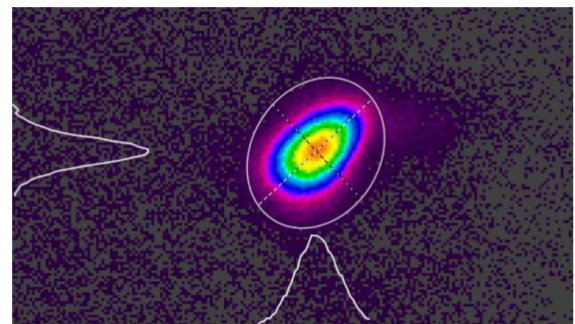


Fig. 2. Pump beam waist spot for the 1064 nm pump light.

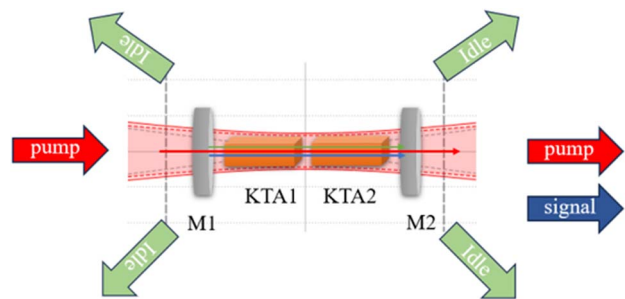


Fig. 3. Optical design of the OPO process.

high pump state. The size of the KTA crystals was $8\text{ mm} \times 8\text{ mm} \times 14\text{ mm}$, and two KTA crystals were placed in the same direction. The cutting angles of the crystals were $\theta = 65.6^\circ$ and $\varphi = 0^\circ$, and the effective nonlinear coefficient d_{eff} was 2.85 pm/V . The acceptance angle of the KTA-OPO for the pump light was no more than $2.88\text{ mrad}\cdot\text{cm}$. The KTA-OPO process adopted a type II angular phase match: $1064.5\text{ nm}(o) \rightarrow 1645.5\text{ nm}(o) + 3014.9\text{ nm}(e)$. Both the pump light and the signal light are p-polarized. All end surfaces of the crystals were HT-coated for the pump, signal, and idler lights (HT@1645 nm, HT@1064 nm, and HT@3015 nm, respectively). The beam waist of the pump light was located at the center of the KTA crystals, and the OPO cavity as a whole was situated inside the Rayleigh distance of the pump light, as shown in Fig. 2, with the left and right grey dashed lines representing the Rayleigh range.

By Gaussian beam simulation with the condition of $\lambda = 1064\text{ nm}$, $M^2 = 1.3$, and the beam waist radius at the x -direction was $161\text{ }\mu\text{m}$, the horizontal Rayleigh distance of the pump light was calculated to be 58.1 mm . The vertical Rayleigh distance of the pump light was calculated to be 136.3 mm by a vertical beam waist radius of $245\text{ }\mu\text{m}$. In order to reduce the threshold of the 1645 nm signal light, it was necessary to place the OPO cavity within the Rayleigh range of the pump light.

The two crystals were fixed by the 3D adjustment frame and a precisely adjustable bracket, which was convenient for precisely adjusting the angle of the KTA crystals. M1 (HR@1645 nm, HT@1064 nm, and HT@3015 nm) was the input mirror of the pump light, and M2 (HT@1064 nm, HT@3015 nm, and $T = 40\%$ @1645 nm) was the output mirror of the signal light. The cavity mirrors were also fixed by the 3D adjustment frame and placed as close to the crystals as possible to reduce the threshold intensity of the OPO oscillation. During the OPO oscillation, the 1645 nm signal light established oscillation after several reflections from the high reflectivity cavity mirror M1 and the 40% transmittance cavity mirror M2. A 3015 nm idler light existed at a walk-off angle of 32.27 mrad , and after passing through the high transmittance M1 and M2, it could not establish an oscillation, so that only the 1645 nm signal light was ultimately single resonant. M3 (45° HR@1645 nm, 45° HT@1064 nm, and 45° HR@3015 nm) and M4 (45° HR@1645 nm, HT@1064 nm, and 45° HT@3015 nm) were used to filter the signal light, and two power meters were used to receive the 1645 nm signal light and the remaining 1064 nm pump light, respectively.

3. Experimental Results and Discussion

As shown in Fig. 4(a), the threshold is 48.6 W at 10 kHz repetition rate. When the pump power increased from 0 to 48.6 W , the 1645 nm output power was observed to be nearly zero. As the pump power increased from 48.6 to 58.8 W , the output power of the 1645 nm signal light exhibited a corresponding rise. Upon reaching the maximum value of 58.8 W for the pump power, the maximum average power of the 1645 nm laser was observed to be 6.35 W . Upon alteration of the repetition rate from

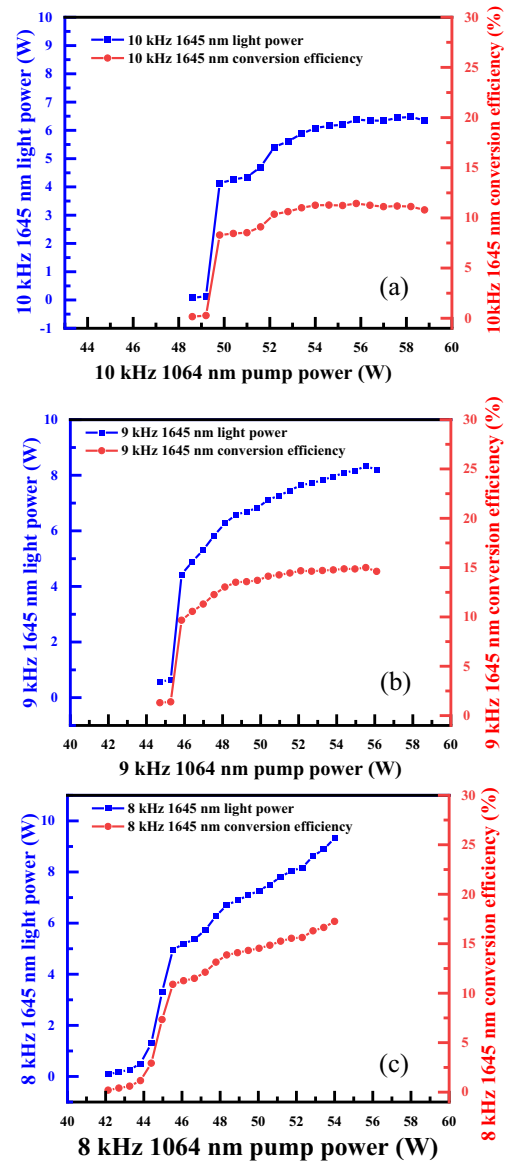


Fig. 4. (a) Variation of the 1645 nm power with the pump power at 10 kHz , (b) variation of the 1645 nm power with the pump power at 9 kHz , and (c) variation of the 1645 nm power with the pump power at 8 kHz .

10 to 9 kHz , the maximum average output power at 1645 nm was observed to be 8.20 W , with a pump power of 56.1 W , as shown in Fig. 4(b). When the repetition rate changed to 8 kHz , the maximum average power of 9.32 W was obtained at 1645 nm when the pump power was 54.1 W , as shown in Fig. 4(c). This corresponded to an optical-optical conversion efficiency of 17.3% . The threshold of the pump light decreased to 42.1 W .

The power stability of the 8 kHz 1645 nm signal light and 8 kHz 1064 nm pump light for 60 min was recorded using power meters connected to the StarLab software, and we obtained the instability of 1.99% @1645 nm and 0.53% @1064 nm, as shown in Fig. 5.

When the pump power increased to 54.1 W at an 8 kHz repetition rate, the temperature of the KTA crystals was observed

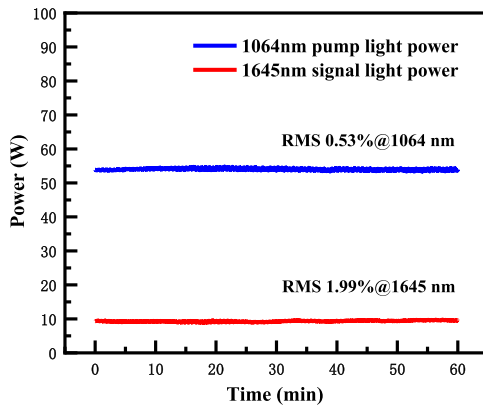


Fig. 5. Power stability of the 1645 nm signal light and the 1064 nm pump light.

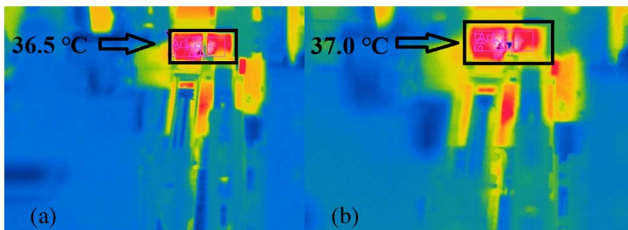


Fig. 6. (a) Thermal imager observation of the temperature of the KTA crystals at $T = 0$ min. (b) Thermal imager observation of the temperature of the KTA crystals at $T = 60$ min.

with a thermal imaging camera at $T = 0$ min and $T = 60$ min while the power stability was measured, as shown in Figs. 6(a) and 6(b). At $T = 0$ min, the temperature of the KTA crystals was 36.5°C . At $T = 60$ min, the temperature of the KTA crystals was 37.0°C . The temperature of the KTA crystals rose only 0.5°C in 60 min, which indicated that the KTA crystals did not accumulate a large amount of heat during the nonlinear process. By monitoring the temperature of the KTA crystals over a long time and combining it with the power stability image, we can conclude that the temperature change of the KTA crystal has almost no effect on the angular phase matching. At the same time, the thermal lensing effect generated by the crystal transforms the planar cavity mirror from a critical cavity to a stable cavity, which achieves a stable signal light output.

We used a silicon photodetector (DET025AFC/M) and an oscilloscope (LECROY wave surfer 104MXs-B) to measure the output 1645 nm pulse waveform. The minimum pulse duration is 1.8 ns, which is shown in Fig. 7(a). The repetition rate of the pulse is 10 kHz, as shown in Fig. 7(b). The pulse width of the experimental pump source was approximately 2.3 ns, while the pulse width of the 1645 nm signal light after OPO was approximately 1.8 ns. A comparison of the pump source pulse and the signal light pulse revealed that the conversion efficiency was low due to the relatively low peak power density in the initial portion of the pulse front. Conversely, the peak power density in the central and posterior sections was high, resulting in a higher

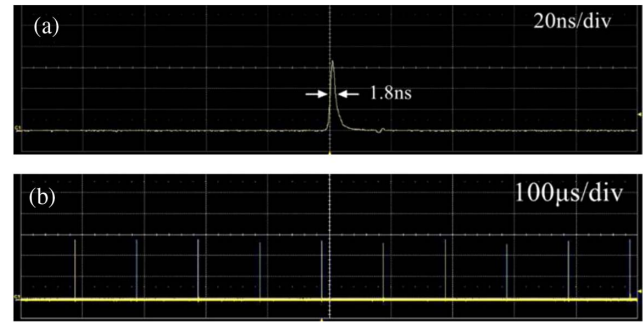


Fig. 7. (a) Pulse duration of the 1645 nm signal light. (b) 10 kHz repetition rate of the 1645 nm signal light.

conversion efficiency. This discrepancy gave rise to a narrowing effect on the time scale. The peak power of the 1645 nm signal light was 735 kW, and the peak power density of the 1645 nm signal light was $8.3\text{ MW}/\text{cm}^2$. The spectrum of the output 1645 nm laser light was measured using a spectrometer (YOKOGAWA, AQ6370D), and we obtained the spectrum with a central wavelength of 1645.2200 nm, as shown in Fig. 8.

Figure 9 shows the phase matching curve of the type II KTA angle obtained by simulation, in which the blue curve represents the change of the signal light wavelength with the phase

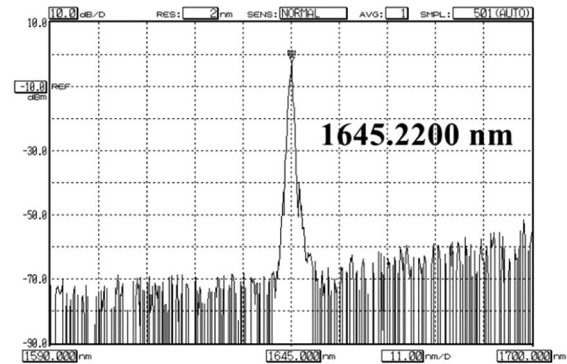


Fig. 8. Spectrogram of the 1645 nm laser spectrum measured by a YOKOGAWA spectrometer.

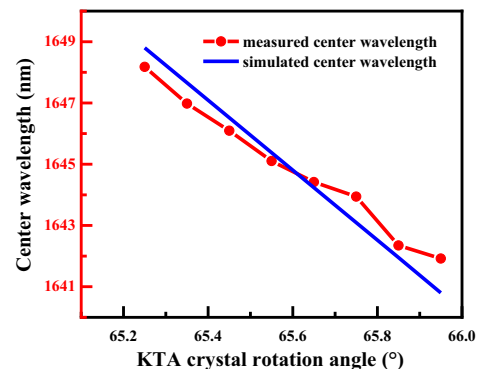


Fig. 9. Relationship between the rotation angle and the tuning wavelength of the KTA crystal.

matching angle. It can be seen that when $\theta = 65.6^\circ$ and $\varphi = 0^\circ$, the signal light wavelength of 1645 nm can be obtained. A specific angle adjustment can continuously change the wavelengths of the output signal light and the idler light by the continuity of the curves.

In the experiment, turning the fine adjustment knob of the crystals' support rods drove the KTA crystals to adjust precisely within a small angle range, and the center wavelength of the output laser can be tuned. For every turn of the support rod, the KTA2 crystal rotated 0.1° in the direction away from the compensation, and the corresponding output center wavelength can be tuned to about 1 nm. Due to the restricted length of the OPO cavity (35 mm) in the experimental setup, the KTA2 crystal's rotation angle in the cavity was limited. The relationship between the KTA crystals' matching angle and the output wavelength is shown by the red line in Fig. 9, and the average wavelength of the KTA-OPO output was continuously tunable from 1641.9207 to 1648.1791 nm. The actual measured continuous tuning curve was found to be consistent with the theoretical calculation.

After generating the 1645 nm signal light, the near-field spot of the 1645 nm signal light was measured by a CCD (Ophir, SP928), as shown in Fig. 10. The near-field spot of the 1645 nm signal light had an ellipticity of 0.9 and a size of $1.723 \text{ mm} \times 1.627 \text{ mm}$, with a TEM₀₀ mode laser output.

Using the beam quality analyzer (Spiricon M2-200 s) to measure the beam quality of the output 1645 nm laser, the beam quality was measured as $M_x^2 = 1.08$ and $M_y^2 = 1.22$, as shown in Fig. 11. The light spot image situated at the center of Fig. 11 represents the intensity distribution of the beam waist, as measured by the M^2 instrument. The distribution was approximately Gaussian in form. The shaping of the pump light had a potential impact on the beam quality of the signal light: if the divergence angle was not the same in the horizontal and vertical directions, it would be difficult to achieve phase matching with the cavity mode of the OPO, which would ultimately lead to a deterioration of the beam quality.

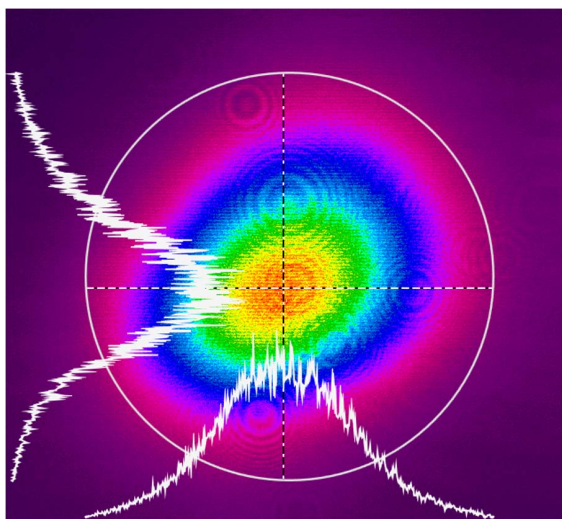


Fig. 10. Near-field spot of the 1645 nm signal light.

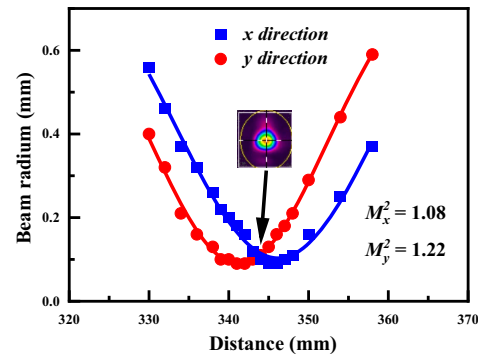


Fig. 11. Beam quality factor of the 1645 nm signal beam measured by the Spiricon M2-200 s.

4. Conclusion

In this Letter, we demonstrate a 1645 nm KTA OPO at a kilohertz nanosecond wavelength. A 1064 nm MOPA laser was used for the pump source, and then Innoslab amplification was applied to produce a 58.8 W 10 kHz 1064 nm pump light. A signal light with a center wavelength of 1645 nm, a repetition rate of 10 kHz, and a power of 6.35 W was then generated by type II angular phase matching. By adjusting the repetition rate of the pump laser, the highest output power of 9.32 W at 8 kHz was obtained, corresponding to an optical-to-optical conversion efficiency of 17.3%. The minimum pulse duration was 1.8 ns with a 735 kW peak power of the signal light. By varying the matching angle of the crystals, we achieved a continuous tunability across a wide wavelength range from 1641.9207 to 1648.1791 nm. The measured beam quality was $M_x^2 = 1.08$ and $M_y^2 = 1.22$. To the best of our knowledge, this is the highest average power achieved at the kilohertz regime of a 1645 nm laser.

References

1. A. Fix, A. Amediek, H. Bovensmann, *et al.*, "CoMet: an airborne mission to simultaneously measure CO₂ and CH₄ using lidar," in *EPJ Web of Conferences* (2018), Vol. 176, p. 02003.
2. S. Nikolov, C. Wuhler, C. Kuhl, *et al.*, "MERLIN: design of an IPDA LIDAR instrument," *CEAS Space J.* 11, 437 (2019).
3. A. Amediek, G. Ehret, A. Fix, *et al.*, "CHARM-F—a new airborne integrated-path differential-absorption lidar for carbon dioxide and methane observations: measurement performance and quantification of strong point source emissions," *Appl. Opt.* 56, 5182 (2017).
4. X. Zhang, M. Zhang, L. Bu, *et al.*, "Simulation and error analysis of methane detection globally using spaceborne IPDA lidar," *Remote Sens.* 15, 3239 (2023).
5. C. Kiemle, M. Quatrevalet, G. Ehret, *et al.*, "Sensitivity studies for a space-based methane lidar mission," *Atmos. Meas. Tech.* 4, 2195 (2011).
6. A. Fix, A. Amediek, C. Budenbender, *et al.*, "CH₄ and CO₂ IPDA LIDAR measurements during the COMET 2018 airborne field campaign," in *EPJ Web of Conferences* (2020), Vol. 237, p. 03005.
7. V. Cassé, F. Gibert, D. Edouart, *et al.*, "Optical energy variability induced by speckle: the cases of MERLIN and CHARM-F IPDA Lidar," *Atmosphere* 10, 540 (2019).
8. M. Bode, M. Alpers, B. Millet, *et al.*, "Merlin: an integrated path differential absorption (IPDA) lidar for global methane remote sensing," *Proc. SPIE* 10563, 1056309 (2014).

9. J. Lohring, J. Luttmann, R. Kasemann, *et al.*, "INNOSLAB-based single-frequency MOPA for airborne lidar detection of CO₂ and methane," *Proc. SPIE* **8959**, 89590J (2014).
10. B. Zhang, X. Dong, J. He, *et al.*, "High-power eye-safe intracavity KTA OPO driven by a diode-pumped Q-switched Nd:YAG laser," *Laser Phys. Lett.* **5**, 12 (2008).
11. L. He, K. Liu, N. Zong, *et al.*, "A high conversion efficiency q-switched intracavity Nd:YVO₄/KTA optical parametric oscillator under direct diode pumping at 880nm," *Chin. Phys. Lett.* **36**, 044202 (2019).
12. H. Chen, H. Huang, S. Wang, *et al.*, "A high-peak-power orthogonally-polarized multi-wavelength laser at 1.6-1.7 μm based on the cascaded non-linear optical frequency conversion," *Opt. Express* **27**, 24857 (2019).
13. K. Liu, L. He, Q. Peng, *et al.*, "A high energy, wavelength and repetition rate tunable eye-safe picosecond optical parametric oscillator," *Laser Phys. Lett.* **16**, 045002 (2019).
14. Y. Yu, Z. Liu, K. Liu, *et al.*, "High-energy picosecond single-pass multi-stage optical parametric generator and amplifier," *Chin. Phys. B* **31**, 014204 (2022).
15. M. Livrozet, F. Elsen, J. Wuppen, *et al.*, "Feasibility and performance study for a space-borne 1645nm OPO for French-German satellite mission MERLIN," *SPIE Lasers* **8959**, 89590G (2014).
16. X. Chen, X. Zhu, S. Li, *et al.*, "Injection-seeded optical parametric oscillator at 1645 nm for space-borne remote sensing of CH₄," *Proc. SPIE* **11185**, 1118547 (2019).